JACC Vol. 32, No. 6
November 15, 1998:1756–64

EXPERIMENTAL STUDIES

Quantification and Time Course of Microvascular Obstruction by Contrast-Enhanced Echocardiography and Magnetic Resonance Imaging Following Acute Myocardial Infarction and Reperfusion

KATHERINE C. WU, MD,* RAYMOND J. KIM, MD,† DAVID A. BLUEMKE, MD, PHD,‡ CARLOS E. ROCHITTE, MD,* ELIAS A. ZERHOUNI, MD,‡ LEWIS C. BECKER, MD,* JOAO A. C. LIMA, MD, FACC*

Baltimore, Maryland and Chicago, Illinois

Objectives. **We aimed to validate contrast-enhanced echocardiography (CE) in the quantification of microvascular obstruction (MO) against magnetic resonance imaging (MRI) and the histopathologic standards of radioactive microspheres and thioflavin-S staining. We also determined the time course of MO at days 2 and 9 after infarction and reperfusion.**

Background. **Postinfarction MO occurs because prolonged ischemia produces microvessel occlusion at the infarct core, preventing adequate reperfusion. Microvascular obstruction expands up to 48 h after reperfusion; the time course beyond 2 days is unknown. Though used to study MO, CE has not been compared with MRI and thioflavin-S, which yield precise visual maps of MO.**

Methods. **Ten closed-chest dogs underwent 90-min coronary artery occlusion and reperfusion. Both CE and MRI were performed at 2 and 9 days after reperfusion. The MO regions by both methods were quantified as percent left ventricular (% LV) mass. Radioactive microspheres were injected for blood flow determination. Postmortem, the myocardium was stained with thioflavin-S and 2,3,5-triphenyltetrazolium chloride.**

Results. **Expressed as % total LV, MO by MRI matched in size MO by microspheres using a flow threshold of <40% remote (4.96 ± 3.52% vs. 5.32 ± 3.98%, p = NS). For matched LV cross sections, MO by CE matched in size MO by microspheres using a flow threshold of <60% remote (13.27 ± 4.31% vs. 13.5 ± 4.94%, p = NS). Both noninvasive techniques correlated well with microspheres (MRI vs. CE, r = 0.87 vs. 0.74; p = NS). Microvascular obstruction by CE corresponded spatially to MRI-hypoenhanced regions and thioflavin-negative regions. For matched LV slices at 9 days after reperfusion, MO measured 12.94 ± 4.51% by CE, 7.11 ± 3.68% by MRI and 9.18 ± 4.32% by thioflavin-S. Compared to thioflavin-S, both noninvasive techniques correlated well (CE vs. MRI, r = 0.79 vs. 0.91; p = NS). Microvascular obstruction size was unchanged at 2 and 9 days (CE: 13.23 ± 4.11% vs. 12.69 ± 4.97%; MRI: 5.53 ± 4.94% vs. 4.68 ± 3.44%; p = NS for both).**

Conclusions. **Both CE and MRI can quantify MO. Both correlate well with the histopathologic standards. While MRI can detect regions of MO with blood flow <40% of remote, the threshold for MO by CE is <60% remote. The extent of MO is unchanged at 2 and 9 days after reperfusion.**

(J Am Coll Cardiol 1998;32:1756–64)

Reperfusion therapy has significantly improved survival following acute myocardial infarction (MI) (1,2). The mortality reduction can be attributed to myocardial salvage (3,4). However, the benefits of late reperfusion are known. Studies support the "open artery hypothesis" (5,6). Nonetheless, clinically, it is difficult to gauge if "optimal reperfusion" has occurred (7). A "patent" infarct-related epicardial coronary artery by angiography is an inadequate marker of tissue-level reperfusion (7,8). This arises from the inhomogeneity of myocardial injury during ischemia which may preclude optimal reperfusion because of microvessel occlusion.

In canines, Kloner et al. (9) demonstrated that 40 min of ischemia, while causing irreversible myocyte injury, is well tolerated by the capillary bed: no serious capillary damage or perfusion defects result. With ischemia beyond 60 min, the infarct core is characterized by injury of the endothelial cells that form the intramyocardial capillaries (9). Examined by electron microscopy, the microvessels are occluded by erythrocytes, neutrophils and debris, such that even with epicardial blood flow restoration, the infarct core will not reperfuse (9,10). This area of microvascular obstruction (MO) is termed the no-reflow region (9,10). Microvascular obstruction occurs in humans and correlates with poorer global left ventricular (LV) function (8,11) and more frequent post-MI complications

From the *Division of Cardiology, Department of Medicine, The Johns Hopkins University School of Medicine, Baltimore, Maryland; the †Division of Cardiology, Department of Medicine, Northwestern University Medical School, Chicago, Illinois; and ‡Division of Diagnostic Imaging, Department of Radiology, The Johns Hopkins University School of Medicine, Baltimore, Maryland.

Supported by Grant-In-Aid #92-10-26-01 of the American Heart Association, Dallas, Texas, and NHLBI grants HL-45090 and P50HL52315 (SCOR in Ischemic Heart Disease), NIH, Bethesda, Maryland.

Manuscript received January 20, 1998; revised manuscript received July 8, 1998, accepted July 29, 1998.

Address for correspondence: Dr. Joao A.C. Lima, The Johns Hopkins Hospital, Division of Cardiology, Blalock 569, 600 North Wolfe Street, Baltimore, Maryland 21287. E-mail: jlima@welchlink.welch.jhu.edu.

0735-1097/98/$19.00
PII S0735-1097(98)0000429-X

Abbreviations and Acronyms

CE = contrast-enhanced echocardiography
LAD = left anterior descending artery
LV = left ventricular
MI = myocardial infarction
MO = microvascular obstruction
MRI = magnetic resonance imaging
TTC = 2,3,5-triphenyltetrazolium chloride

(11,12). It thus has important prognostic significance after acute MI.

Experimentally, radioactive microspheres have been the "gold standard" for determining MO. Areas of MO have been defined as regions with blood flow rates below 50% of the remote region after reperfusion (13). Thioflavin-S has also been used to depict MO (9,10) because it provides a precise visual map of MO extent. Both methods, however, require postmortem evaluation, precluding the serial examination of MO in the same animal and application to humans. Recently, the noninvasive technique of contrast-enhanced magnetic resonance imaging (MRI) was able to depict MO (12,14–16) and validated against the histopathologic standards (15,16). While contrast echocardiography (CE) has also been used to assess microvascular integrity (8,11,17), its spatial location and extent have not been validated against the histopathologic standards or MRI. This study was designed to investigate this aspect.

Until recently, MO was felt to be fully established during coronary occlusion, hence the term "no-reflow". However, the MO region has been shown to nearly triple in size from 2 min to 3.5 h after reperfusion (10). Using MRI and radioactive microspheres, we have shown further MO augmentation up to 48 h after reperfusion (18). The extent of MO beyond 2 days is unknown. The temporal course of MO is important because interventions that limit MO could improve post-MI prognosis and add to the understanding of MI pathophysiology. Thus, the validation of noninvasive techniques to quantify MO is crucial.

Our study goals were as follows: 1) to validate the extent and spatial location of MO by CE against the histopathologic standards of microsphere blood flow and thioflavin-S; 2) to compare the abilities of CE and MRI to quantify MO serially; and 3) to use CE and MRI to further characterize the time course of MO up to 9 days after infarction.

Methods

Experimental preparation. Ten mongrel dogs were studied. Experiments conformed to the "Position of the American Heart Association on Research Animal Use" adopted in 1984.

Experimental myocardial infarction. Animals were anesthetized and mechanically ventilated. Catheter sheaths were placed in the right femoral artery and vein and in the carotid artery. A 7F pigtail catheter was placed in the LV for radioactive microsphere administration and pressure monitoring. Three thousand units of intravenous heparin was given. A 2.5-cm angioplasty balloon was inflated to occlude the left anterior descending artery (LAD) for 90 min and then deflated for reperfusion. Both LAD occlusion and postreperfusion patency were shown angiographically. The animals were allowed to recover.

Day 2 after MI. Animals were anesthetized and mechanically ventilated. Sheaths were placed in the left femoral vessels. A pigtail catheter was placed in the LV for microsphere administration and hemodynamic measurements.

Day 9 after MI. The protocol was similar to day 2, except that the left carotid and jugular vessels were used.

Radioactive microspheres. Microspheres were used to measure regional blood flow. For each measurement, ≈2,000,000 sonicated microspheres (15 ± 1 μm) labeled with ^{153}Gd, ^{113}Sn, ^{103}Ru, ^{95}Nb or ^{46}Sc (DuPont) were injected into the left ventricle. Starting before microsphere injection and continuing for 2 min thereafter, arterial blood samples were withdrawn at a rate of 2.06 ml/min. Flow was determined at five time points: baseline, preceding coronary occlusion, 70 min after coronary occlusion, and 30 min, 2 days and 9 days after reperfusion.

Contrast-enhanced echocardiography protocol. Contrast-enhanced echocardiography was performed at days 2 and 9 after MI, after microsphere injections but before MRI, in seven dogs. Animals were placed in the left lateral decubitus position. Images were obtained with a Hewlett-Packard Sonos 500, 2.5 MHz transducer. At the first imaging session for each animal, gain settings were optimized and maintained throughout the protocol. At each session, two end diastolic short-axis images, one at the midpapillary muscle level and one at the midventricular level, were obtained. Imaging began ≈20 s before contrast injection and continued for ≈45 to 60 s. Three to five milliliters of Albunex (Mallinckrodt Medical, Inc.) were bolus injected into a 7F pigtail catheter positioned in the aortic outflow tract just distal to the valve leaflets.

MRI protocol. Images were acquired at 2 and 9 days after MI using a 1.5T whole body magnet (Signa, General Electric) and the contrast agent, Magnevist (gadopentetate dimeglumine, Berlex Laboratories). Animals were placed in the left lateral decubitus position with a flexible radiofrequency coil (GP-FLEX) wrapped around the chest. We used a fast gradient-echo imaging pulse sequence, SPGR (Spoiled Gradient Recall Acquisition in Steady State-GRASS) (19). Parameters were matrix size = 256 × 108, field of view = 32 cm, TR = 6.5 ms, TE = 2.3 ms, flip angle = 45° and voxel size = 1.2 mm × 3.3 mm × 10.0 mm. Middiastolic images were acquired during mechanical ventilation cessation. Breathholds lasted 20 to 30 s. Between breathholds, animals were ventilated for 30 s. The protocol began with a venous injection of Magnevist (0.225 mmol/kg), continuing for 15 min thereafter. One third of k space was acquired during each cardiac cycle (central third acquired first, 36 phase-encodes/heartbeat), with four to five base-to-apex short-axis cross sections imaged four times/breathhold.

Contrast-enhanced echocardiography data analysis. Images were analyzed without postprocessing by two observers

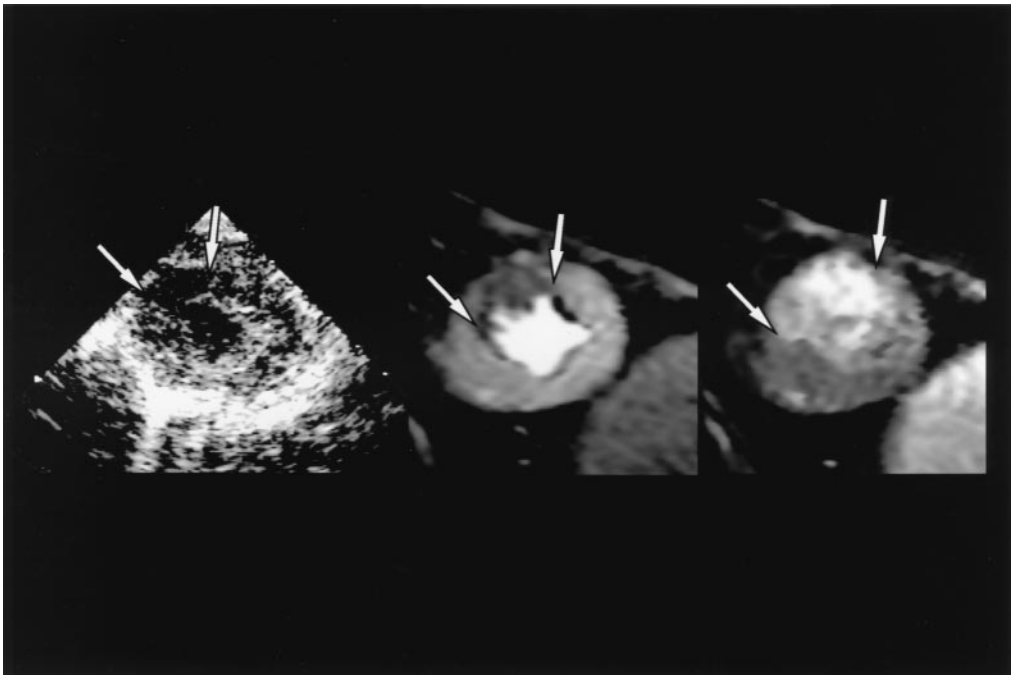

Figure 1. Corresponding CE and MR images. The CE defect matches in spatial extent the MRI hypoenhanced region. Both the CE defect and MRI hypoenhanced region are in the same location as the MRI hyperenhanced area, but are smaller.

blinded to MRI and postmortem data. Images early after contrast injection, that is, within 10 cardiac cycles, were chosen. For each slice, the contrast defect, endocardial and epicardial contours were planimetered with the aid of computer software (Sigma-Scan-V3.90, Jandel Scientific). The contrast defect was expressed as percent LV (% LV) myocardial area in that slice. MO quantification by CE was compared to MRI (Fig. 1) and thioflavin-S on a slice-by-slice basis. Because the entire LV was imaged by MRI and studied by histopathologic methods, the slices which best matched the CE cross sections were chosen using anatomical landmarks (i.e., papillary muscles and right ventricular insertions). To assess MO time course, the two CE slices from day 2 were compared with corresponding slices from day 9.

Magnetic resonance imaging data analysis. Images were analyzed sequentially from baseline, before contrast, to 15 min after contrast injection with software package NIH IMAGE (National Institutes of Health, Bethesda, Maryland). Three patterns of myocardial signal enhancement were identified, as earlier described (14,15). In noninfarcted myocardium, signal intensity rises rapidly in the first minute after contrast injection and then decays over 10 to 15 min. Infarcted myocardium generates signal that also rapidly gains in intensity during the first minute after contrast but which continues to increase for 2 to 3 min before slowly decaying. This causes hyperenhancement of infarcted relative to normal myocardium during the 10 to 15 min after contrast injection. The third pattern is that of a gradual increase in signal intensity over the first 3 min after contrast injection. Such areas are hypoenhanced relative to surrounding myocardium and correspond to regions of MO or "no reflow" (15,16,18). Hypoenhancement persists for ≈1 min and is located in the subendocardium of the infarct core.

Microvascular obstruction extent. The MO region was identified from early images showing distinct hypoenhancement persisting for ≥1 min. The hypoenhanced area was planimetered for each base-to-apex short-axis slice. Microvascular obstruction extent, expressed as % total LV mass, was calculated based on the percent of hypoenhancement in each slice, weighted according to slice cross-sectional area. For all slices, MO size = Σ(% hypoenhanced)(cross-sectional area)/Σ(cross-sectional area).

Infarct size. The hyperenhanced region was identified from images obtained 5 to 10 min after contrast. The area of hyperenhancement was planimetered for each base-to-apex short-axis slice. Infarct size, expressed as % total LV mass, was calculated based on the percent of hyperenhancement in each slice, weighted according to slice cross-sectional area. Thus, for all slices, infarct size = Σ(% hyperenhanced)(cross-sectional area)/Σ(cross-sectional area).

Postmortem measurement of MO, infarct and risk regions. *Microvascular obstruction and infarct size.* After day 9 imaging, 20 ml of 4% thioflavin-S solution was injected into the left ventricle. The hearts were then arrested with potassium chloride and excised. The epicardial fat, atria, right ventricular free wall and valvular apparatus were removed. The left ventricle was sectioned into four to five short-axis slices. Each slice (apical side) was viewed under ultraviolet light and the thioflavin-negative (MO) region (9,10) and myocardial borders were traced on clear acetate sheets. The slices were incubated in 2,3,5-triphenyltetrazolium chloride (TTC) 2% solution for 20 min at 37°C. They were then viewed under room light to

Table 1. Hemodynamic Measurements

	Baseline	Occlusion (70 min)	Reperfusion (30 min)	Reperfusion (Day 2)	CE (Day 2)	Reperfusion (Day 9)	CE (Day 9)
Systolic BP (mm Hg)	128 ± 13	111 ± 13	111 ± 17	118 ± 14	122 ± 17	106 ± 8	107 ± 17
Diastolic BP (mm Hg)	91 ± 12	77 ± 14	74 ± 13	76 ± 15	76 ± 17	76 ± 11	80 ± 16
Mean BP (mm Hg)	103 ± 12	88 ± 14	87 ± 14	90 ± 13	91 ± 17	86 ± 9	89 ± 15
Heart rate (beats/min)	115 ± 15	107 ± 17	101 ± 24	118 ± 22	120 ± 20	115 ± 15	103 ± 8

Abbreviations: BP = blood pressure; CE = contrast-enhanced echocardiography.

delineate the TTC-negative (infarcted) region (20) which was traced on clear acetate sheets. From the drawings, the thioflavin-negative, TTC-negative and LV myocardial areas were planimetered (Sigma-Scan-V3.90, Jandel Scientific) for each slice. MO extent and infarct size were calculated as % total LV mass: % region of interest = Σ(% region of interest)(cross-sectional area)/Σ(cross-sectional area).

Microsphere blood flow analysis. After MO and infarct size determination, the LV slices were sectioned into pie-shaped wedges which were then subdivided into five equal regions from endocardium to epicardium, yielding ≈350 myocardial samples/heart. Each sample was weighed, its location recorded and then counted in a gamma emission well spectrometer (Cobra II, Hewlett-Packard). Regional blood flow was calculated by standard methods (21,22).

To calculate blood flow, myocardial samples were grouped into four regions: remote (LV wall opposite that of the infarct); thioflavin-negative (MO); thioflavin-positive/TTC-negative (infarcted); and noninfarcted risk (TTC-positive with blood flow <50% of remote during coronary occlusion). The risk region, expressed as % total LV weight, was quantified by summing the weights of all samples with blood flow <50% of remote during coronary occlusion.

The extent of regions receiving blood flow <40%, <50% and <60% of remote was also determined at days 2 and 9 after MI. The weights of all myocardial samples contained within the TTC-negative region with flow below a defined threshold (i.e., 40%, 50% or 60%) were summed and expressed as % total LV weight both on a slice-to-slice basis and for the entire left ventricle.

Statistical analysis. Microvascular obstruction extents by the various methods were compared with repeated-measures one-way analysis of variance (23). Differences between pairs of methods were isolated with Bonferroni t tests (23). Linear regression analyses (24) were used to compare the methods of quantifying MO and infarct size. Serial changes in MO extent, infarct size and regional blood flow were compared with paired t tests (23). Fisher's z transformation (24) was used to test pairs of correlation coefficients. Results are reported as mean ± SD with p values <0.05 considered significant.

Results

Hemodynamics. Table 1 summarizes the hemodynamic measurements observed during the protocol. The changes were typical of those seen during acute MI and reperfusion. As documented previously, Albunex did not significantly alter hemodynamics (25).

Myocardial blood flow. Figure 2 shows myocardial blood flow rates (relative to remote areas) in the regions of 1) MO (thioflavin-negative) and 2) infarcted with patent microvasculature (thioflavin-positive/TTC-negative). At baseline, the regions had similar flow. With occlusion, flow to both regions declined ($p < 0.01$). As expected, region 1 (MO) had lower

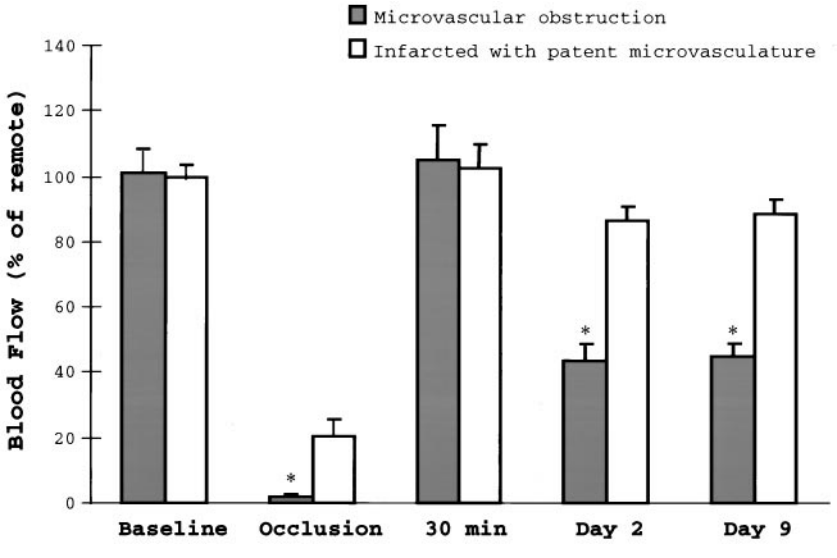

Figure 2. Regional blood flow. The asterisk denotes the significant difference in flows between MO and infarcted (microvasculature intact) regions at the same timepoint. Microvascular obstruction and infarcted regions had similar baseline flows. At occlusion, flow to MO regions was lower than to regions that become infarcted but whose microvasculatures remain intact ($p = 0.0002$). With reperfusion, blood flow in both regions returns to baseline. At day 2, MO regions have lower blood flow than infarcted areas ($p < 0.0001$). At day 9, MO regions continue to have flow that is lower than infarcted areas ($p < 0.0001$). Within each region, flow rates at days 2 and 9 are similar (p = NS).

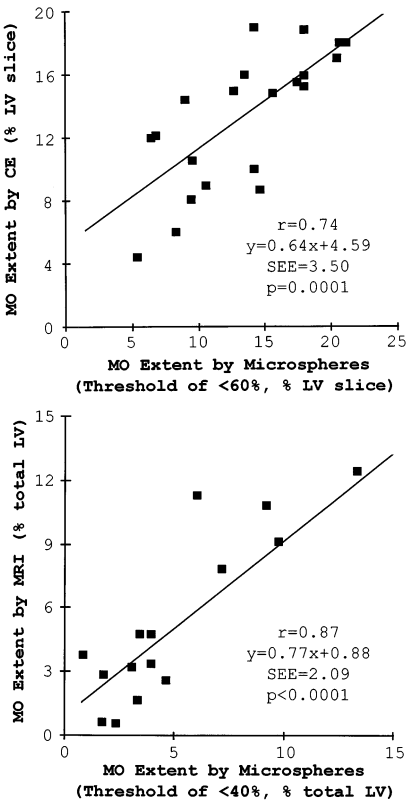

Figure 3. Correlation between MO by noninvasive techniques versus radioactive microspheres.

flow (p = 0.0002) than region 2 (infarcted territory outside the MO region). Thirty minutes after reperfusion, flow to both regions returned to levels similar to baseline (p = NS), indicating successful reperfusion. At 2 days after reperfusion, both regions had flow rates below baseline ($p < 0.004$ for both). Region 1 (MO) had lower flow than region 2 at 2 days ($p < 0.0001$). By 9 days after reperfusion, both regions continued to have flow below baseline ($p < 0.007$ for both). Region 1 (MO) had lower flow than region 2 at 9 days ($p < 0.0001$). Flow to region 1 (MO) was similar at 2 and 9 days after reperfusion (p = NS), as was flow to region 2 (p = NS).

Quantification of MO by microspheres—comparison with MRI, CE and thioflavin-S. Microvascular obstruction by MRI (% total LV) measured 4.96 ± 3.52% versus microsphere-determined areas of 5.32 ± 3.98% (flow threshold of <40% of remote), 7.49 ± 4.54% (threshold of <50%) and 10.57 ± 5.62% (threshold of <60%). Microvascular obstruction by MRI was similar in extent to regions with <40% of remote flow (p = NS), but smaller than areas with <50% (p = 0.001) and <60% ($p < 0.0001$). Microvascular obstruction by MRI correlated with MO by microspheres (Fig. 3).

For matched LV cross sections, MO by CE measured 13.27 ± 4.31% versus microsphere-determined regions of 6.62 ± 4.61% (threshold of <40% of remote flow), 9.51 ± 4.45% (threshold of <50%) and 13.5 ± 4.94% (threshold of <60%). Microvascular obstruction by CE was larger than areas with <40% ($p < 0.0001$) and <50% (p = 0.0001) of remote flow. Microvascular obstruction by CE was similar in size to regions with <60% of remote flow (p = NS). Microvascular obstruction by CE correlated with MO by microspheres (Fig. 3).

For the total left ventricle, MO extent by thioflavin-S was 9.05 ± 5.48% compared with 5.67 ± 3.89% (threshold of <40%), 8.01 ± 4.55% (threshold of <50%) and 11.33 ± 5.25% (threshold of <60%). Microvascular obstruction by thioflavin was larger than regions with <40% (p = 0.0018), smaller than regions with <60% (p = 0.0092) and similar in size to regions with <50% (p = NS) of remote flow. Microvascular obstruction by thioflavin correlated well with MO by microspheres ($r = 0.96$, $y = 1.16\times-0.22$, SEE = 2.17, p = 0.0001).

The correlation between MRI and microspheres (r = 0.87) was similar to (p = NS) that between CE and microspheres (r = 0.74). In contrast, the correlation between CE and microspheres was less robust than that between thioflavin-S and microspheres (r = 0.74 vs. 0.96, p = 0.0244). The correlation between MRI and microspheres versus thioflavin and microspheres was statistically similar (r = 0.87 vs. 0.96, p = NS).

Quantification of MO by CE, MRI and thioflavin-S. Figure 4 shows two typical CE images with corresponding MR images and thioflavin-stained slices. The spatial location of the CE defects correlates with the MRI hypoenhanced and the thioflavin-negative regions.

For matched LV cross sections at day 9 after MI, MO measured 12.94 ± 4.51% by CE, 7.11 ± 3.68% by MRI and 9.18 ± 4.34% by thioflavin (repeated-measures analysis of variance, $F = 22.8$, $p < 0.001$). Microvascular obstruction by CE was larger than by MRI ($t = 6.63$, $p < 0.001$) and by thioflavin-S ($t = 4.41$, $p < 0.001$). Microvascular obstruction by MRI was smaller than by thioflavin-S ($t = 2.21$, $0.01 < p < 0.025$).

For matched slices, MO by CE correlated with thioflavin-S but overestimated it by 68% (Fig. 5). Compared to MO by CE for matched slices, MO by MRI was 60% as large and was modestly correlated (Spearman $r = 0.63$, $y = 0.68\times+7.76$, SEE = 7.03, p = 0.0017). When calculated as % total LV mass, extent of MRI MO (5.42 ± 3.62%) was 61% of thioflavin-S (9.00 ± 4.84%) and the two were well correlated (Fig. 5). Compared to the correlation between MRI and thioflavin, the correlation between CE and thioflavin was similar (r = 0.91 vs. 0.79, p = NS).

Infarct size by MRI and 2,3,5-triphenyltetrazolium chloride. Infarct size (% total LV mass) was 24.97 ± 9.28% by MRI and 18.40 ± 8.38% by 2,3,5-triphenyltetrazolium chloride (TTC). The risk region by microspheres was 41.20 ± 8.34%. For measuring infarct size, MRI and TTC correlated well ($r = 0.91$, $y = 1.01\times+6.36$, SEE = 2.65, p = 0.0002). Relative to the risk region, MRI infarct size was 55% as large and was highly correlated (Spearman's $r = 0.97$, $y = 0.89\times-13.3$, SEE = 6.87, $p < 0.0001$). The TTC region was 42% of the risk

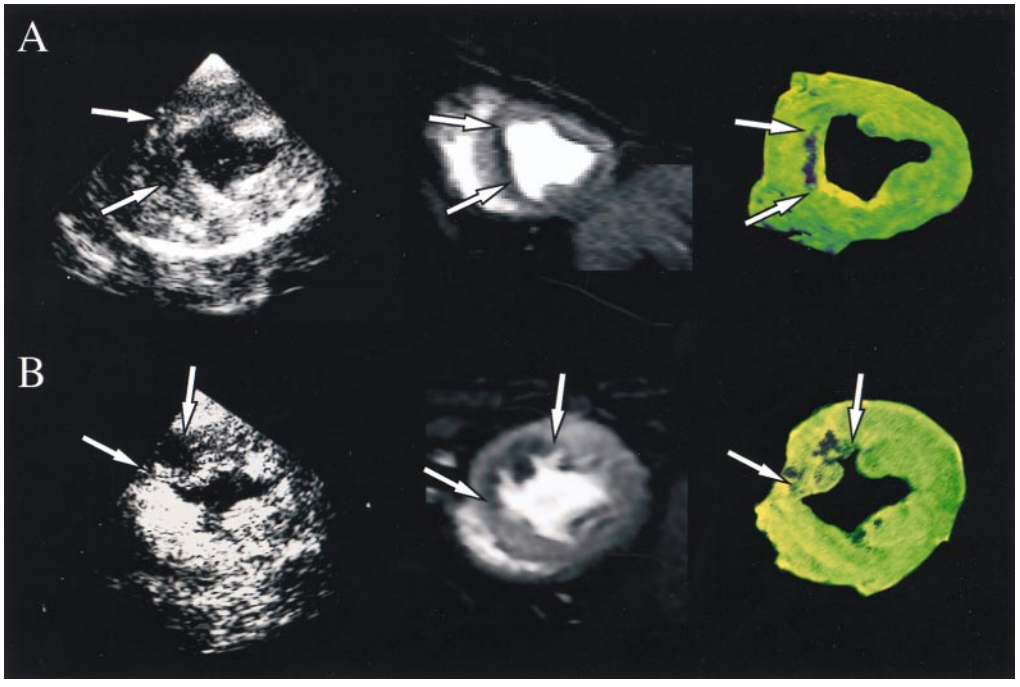

Figure 4. The CE images from separate animals (**A** and **B**) are compared to matched MR images and postmortem thioflavin-S stained slices. The CE defects correspond in location to MO defined by MRI hypoenhancement and thioflavin-negative regions.

region and correlated well (Spearman's r = 0.93, y = 0.92×−20.2, SEE = 8.94, p < 0.002).

Microvascular obstruction extent and infarct size at 2 and 9 days after MI. Figure 6 depicts the time course of MO extent by CE and MRI. The extent of MO (% LV cross-sectional area) by CE was 13.23 ± 4.11% and 12.69 ± 4.97% (p = NS) at 2 and 9 days after MI. By MRI, MO extent (% total LV mass) was 5.53 ± 4.94% and 4.68 ± 3.44% (p = NS). Similarly, infarct size by MRI (% total LV mass) did not change significantly (Fig. 6), measuring 28.41 ± 6.71% and 25.78 ± 9.46% at 2 and 9 days (p = NS).

Microsphere-determined regions of MO (% total LV) did not change over time. At 2 versus 9 days, the MO region was 4.98 ± 3.44% versus 4.70 ± 2.98% (p = NS) using a threshold of <40%; 7.47 ± 4.43% versus 6.93 ± 3.85% (p = NS) for a threshold of <50%, and 10.34 ± 5.98% versus 9.53 ± 4.49% (p = NS) for a threshold of <60%.

Discussion

To our knowledge, this is the first study to directly quantify the extent of postinfarction MO by CE and compare it with the methods of radioactive microspheres and thioflavin-S and with contrast-enhanced MRI. This is also the first investigation of MO time course beyond 3 days after coronary occlusion and reperfusion (26). Microvascular obstruction by CE corresponds in spatial location to MO by MRI and thioflavin. However, the size of the regions differ: MO by CE is larger than MO by thioflavin, which in turn is larger than MO by MRI. The size differentials can be explained by corresponding microsphere "maps" which quantify the extent of regions with varying thresholds of blood flow. While MRI detects a region of MO receiving blood flow <40% of remote, the threshold for

Figure 5. Correlation between MO by noninvasive techniques versus thioflavin-S.

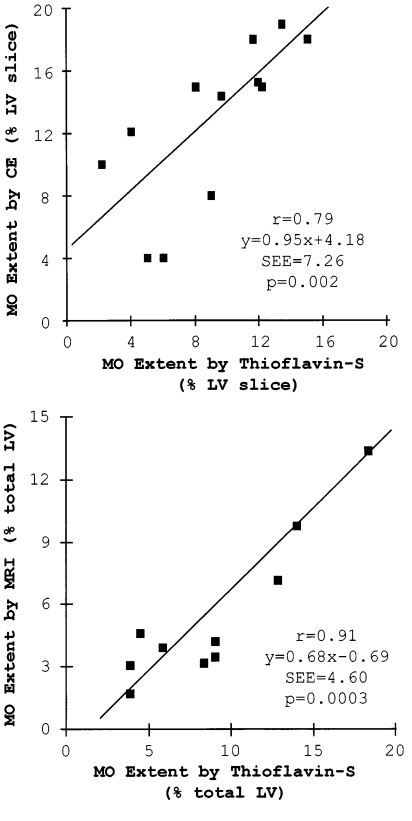

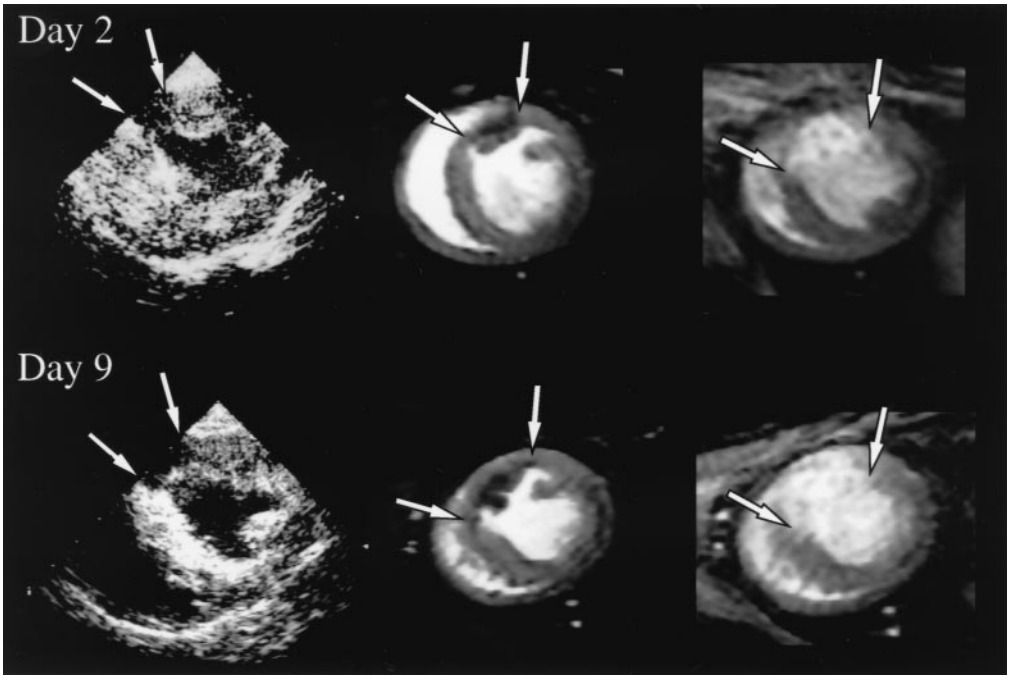

Figure 6. The CE and MR images from the same animal at 2 and 9 days after reperfusion. The CE defects correspond spatially to the regions of MRI hypoenhancement; both do not significantly change over time. The region of MRI hyperenhancement (infarct size) is larger than MO and also does not change over time.

CE detection is <60% of remote. The threshold for lack of thioflavin-S uptake is <50% of remote. Despite the disparity in thresholds, CE and MRI correlated equally well with radioactive microspheres in MO quantification. However, CE correlated less well with microspheres than did thioflavin-S. In contrast, MRI correlated equally well with microspheres as thioflavin-S. Lastly, though MO size expands up to 48 h after reperfusion, as documented previously (10,18), this study shows that at 2 and 9 days after reperfusion, MO extent is similar.

Rationale for differences between CE and MRI. Although both CE and MRI can effectively measure MO, they have different thresholds for detecting flow reduction. Several potential explanations exist. Gadolinium rapidly extravasates from the blood pool into the interstitium and hence, is an interstitial agent. Microbubbles, however, are purely intravascular. Because gadolinium can penetrate into extravascular spaces and travel where bubbles cannot, one may thus expect MRI hypoenhancement to be smaller than the CE defect. Different physical properties of the agents may also contribute. Albumin microbubbles are, on average, larger than gadolinium molecules. Moreover, Albunex is a heterogeneous population of bubbles with variable diameters (27), while gadolinium molecules are uniform. As such, microbubbles larger than gadolinium molecules could become temporarily lodged in microvessels that would allow passage of gadolinium. Thus, the region void of Albunex bubbles should theoretically be larger than the MRI hypoenhanced region. It is also possible that differences in perception threshold underlie disparities in MO measurement. Similar to our findings, Judd et al. (15) showed that MO by MRI corresponded in size to regions with blood flow much less than that measured by thioflavin-S. Given the similar molecular weights of gadolinium and thioflavin-S, the discrepancy between the techniques may be one of perception threshold: a higher concentration of thioflavin-S may be required before the myocardium appears fluorescent (i.e., well-perfused). Analogously, compared to gadolinium, more Albunex microbubbles may be needed to enhance myocardium and hence, there is a higher threshold for distinguishing between normal and underperfused regions by CE.

Ultrasound destruction of microbubbles has been reported (28). Larger CE defects may theoretically result from this phenomenon. This effect, however, is minimal with intraaortic root contrast injections (28), which was the route used in our study. On the other hand, intracoronary Albunex can attenuate images because of high microbubble concentrations. We minimized this with intraaortic root injections and optimal Albunex dosing. Nonetheless, our results are likely specific for the particular contrast agent used. The extent of MO will depend on the size distribution of the microbubble population. Other agents have many more bubbles measuring 5 to 15 μm in diameter compared with Albunex (27). These larger microbubbles may theoretically become temporarily lodged in microvessels and prevent the passage of the smaller microbubbles, creating a measured CE defect that is larger than that of Albunex.

Study limitations. Advances in technology may enhance the ability of CE to quantify MO. Our CE protocol used fundamental imaging and no data postprocessing. Although harmonic imaging improves the signal-to-noise ratio (29,30), it

is not always appreciably different from fundamental imaging (e.g., infarct size measurement [30]). We also used intraaortic root injections of Albunex. Contrast agents which limit pulmonary elimination (27,31,32), coupled with harmonic imaging and continuous contrast administration (33), may improve the accuracy of MO detection and perhaps allow its quantification from intravenous contrast injections.

A second limitation lies in the method by which imaging and histopathologic data were cross registered. Methods of cross registering images obtained by different techniques are suboptimal because of disparities in magnification. While we superimposed transparencies of the CE images, MR images and histopathologic drawings to ensure qualitative concordance of the MO regions, quantitative comparisons were performed as described, in keeping with methodology utilized previously by our group (18).

Advantages of MRI. This study highlights several advantages of MRI. Magnetic resonance imaging allows precise multislice imaging, enabling one to measure MO relative to the entire left ventricle. In contrast, imaging more than two anatomically unique slices by CE is difficult and thus, MO by CE cannot be accurately measured for the whole left ventricle. Regions of MO by MRI are also visually more distinct. Because of greater spatial resolution, MRI can better define the borders of the MO region. Lastly, infarct size is readily available with MRI: hyperenhanced regions correspond to infarcted areas (14,15). With CE, coronary vasodilators are required for infarct size estimation (30).

Contrast-enhanced echocardiography versus MRI. It is unclear whether MO quantification is "better" by CE or by MRI. Contrast-enhanced echocardiography detects a less severe flow reduction than MRI. As markers for degree of microvascular damage, CE can perhaps be seen as more sensitive and MRI as more specific. Within the infarct core, Ambrosio et al. (10) noted severe endothelial cell injury and intracapillary erythrocyte stasis. In adjacent regions, less damaged endothelial cells were interspersed with areas with normal microvessels (10). Hence, the infarct core is likely characterized by complete microvessel occlusion. Surrounding it are rims of tissue that have progressively less obstructed microvessels with gradual interspersion of areas with normal microvasculature. Contrast-enhanced echocardiography may thus detect lesser degrees of microvascular damage than MRI. Nonetheless, this difference may not be clinically important. The prognostic value of MO size may lie in the relative areas by one technique: a large MO region by either CE or MRI may portend a poorer prognosis than a small region by the same technique. Further studies are needed.

Microvascular obstruction time course. The other finding of our study is that the process causing MO expansion early after reperfusion stabilizes between days 2 and 9 after reperfusion. As we quantitated MO at only two timepoints, we cannot definitively plot the course of MO extent between days 2 and 9. Indirect evidence, however, suggests that MO extent recedes after day 9. We previously studied patients by MRI 6 months after MI (12). No patients who had MO by MRI acutely after infarct had evidence of it on 6-month follow-up. Thus, by 6 months, the region of MO has resolved.

With the results of this study and prior work (10,18), one may postulate the time course of MO extent after infarction and reperfusion as progressively increasing, peaking at 2 days after MI; plateau and stabilization in the week thereafter; and gradual recanalization of occluded microvessels causing a progressive decline with eventual disappearance of MO during infarct healing. Implications of this proposed time course for future investigations are numerous. Strategies to prevent MO or hasten its regression may improve prognosis by limiting post-MI remodeling and accelerating infarct healing. Such studies could add insight into the pathophysiologic mechanisms of acute coronary thrombosis and reperfusion.

Conclusions. Both CE and MRI can quantify MO. They are both potentially useful techniques for serially measuring MO extent. They differ in their thresholds to detect reduction in blood flow. With either imaging technique, however, the extent of MO remains unchanged at 2 and 9 days after MI. Therefore, in assessing post-MI prognosis, MO can be studied noninvasively up to at least 1 week after acute MI.

References

1. ISIS-2 (Second International Study of Infarct Survival) Collaborative Group. Randomized trial of intravenous streptokinase, oral aspirin, both or neither among 17,187 cases of suspected acute myocardial infarction: ISIS-2. Lancet 1988;2:349–60.
2. Grines CL, Browne KF, Marco J, et al. A comparison of immediate angioplasty with thrombolytic therapy for acute myocardial infarction. N Engl J Med 1993;328:673–9.
3. Gersh BJ, Anderson JL. Thrombolysis and myocardial salvage: results of clinical trials and the animal paradigm—paradox or predictable? Circulation 1993;88:296–306.
4. Sheehan FH, Doerr R, Schmidt WG, et al. Early recovery of left ventricular function after thrombolytic therapy for acute myocardial infarction: an important determinant of survival. J Am Coll Cardiol 1988;12:289–300.
5. Hochman JS, Choo H. Limitation of myocardial infarct expansion by reperfusion independent of myocardial salvage. Circulation 1987;75:299–306.
6. Nidorf SM, Siu SC, Galambos G, Weyman AE, Picard MH. Benefit of late coronary reperfusion on ventricular morphology and function after myocardial infarction. J Am Coll Cardiol 1993;21:683–91.
7. Lincoff AM, Topol EJ. Illusion of reperfusion: does anyone achieve optimal reperfusion during acute myocardial infarction? Circulation 1993;87:1792–805.
8. Ito H, Tomooka T, Sakai N, et al. Lack of myocardial perfusion immediately after successful thrombolysis. Circulation 1992;85:1699–705.
9. Kloner RA, Ganote CE, Jennings RB. The "no-reflow" phenomenon after temporary occlusion in the dog. J Clin Invest 1974;54:1496–508.
10. Ambrosio G, Weisman HF, Mannisi JA, Becker LC. Progressive impairment of regional myocardial perfusion after restoration of postischemic blood flow. Circulation 1989;80:1846–61.
11. Ito H, Maruyama A, Iwakura K, et al. Clinical implications of the "no reflow" phenomenon: a predictor of complications and left ventricular remodeling in reperfused anterior wall myocardial infarction. Circulation 1996;93:223–8.
12. Wu KC, Zerhouni EA, Judd RM, et al. The prognostic significance of microvascular obstruction by magnetic resonance imaging in patients with acute myocardial infarction. Circulation 1998;97:765–72.
13. Krug A, De Rochemont WM, Korb G. Blood supply of the myocardium after temporary coronary occlusion. Circ Res 1966;19:57–62.
14. Lima JAC, Judd RM, Bazille A, Schulman SP, Atalar E, Zerhouni EA. Regional heterogeneity of human myocardial infarcts demonstrated by contrast-enhanced MRI. Circulation 1995;92:1117–25.

15. Judd RM, Lugo-Olivieri CH, Arai M, et al. Physiological basis of myocardial contrast enhancement in fast magnetic resonance images of 2-day-old reperfused canine infarcts. Circulation 1995;92:1902–10.
16. Kim RJ, Chen EL, Lima JAC, Judd RM. Myocardial Gd-DTPA kinetics determine MRI contrast enhancement and reflect the extent and severity of myocardial injury after acute reperfused infarction. Circulation 1996;94: 3318–26.
17. Ragosta M, Camarano G, Kaul S, Powers ER, Sarembock IJ, Gimple IW. Microvascular integrity indicated myocellular viability in patients with recent myocardial infarction: new insights using myocardial contrast echocardiography. Circulation 1994;89:2562–9.
18. Rochitte CE, Lima JAC, Bluemke DA, et al. The magnitude and time course of microvascular obstruction and tissue injury after acute myocardial infarction. Circulation 1998;98:1006–14.
19. Judd RM, Reeder SB, Atalar E, McVeigh ER, Zerhouni EA. A magnetization-driven gradient echo pulse sequence for the study of myocardial perfusion. Magn Reson Med 1995;34:276–82.
20. Fishbein MC, Meerbaum S, Rit J, et al. Early phase acute myocardial infarct size quantification: validation of the triphenyl tetrazolium chloride tissue enzyme staining technique. Am Heart J 1981;101:593–600.
21. Domenech RJ, Hoffman JIE, Noble MIM, Saunders KB, Henson JR, Subijanto S. Total and regional coronary blood flow measured by radioactive microspheres in conscious and anesthetized dogs. Circ Res 1969;25:581–96.
22. Heymann MA, Payne BD, Hoffman JIE, Rudolph AM. Blood flow measurements with radionuclide-labeled particles. Prog Cardiovasc Dis 1977;20:55–79.
23. Winer BJ. Statistical Principles in Experimental Design. 2nd ed. New York: McGraw-Hill, 1971:351–9.
24. Dawson-Saunders B, Trapp RG. Basic and Clinical Biostatistics. 2nd ed. Norwalk, CT: Appleton & Lange, 1994:161–83.
25. Ten Cate FJ, Widimsky P, Cornel JH, Waldstein DJ, Serruys PW, Waaler A. Intracoronary Albunex: its effects on left ventricular hemodynamics, function, and coronary sinus flow in humans. Circulation 1993;88(part 1):2123–7.
26. Cobb FR, Bache RJ, Rivas F, Greenfield JC Jr. Local effects of acute cellular injury on regional myocardial blood flow. J Clin Invest 1976;57:1359–68.
27. Skyba DM, Camarano G, Goodman NC, Price RJ, Skalak TC, Kaul S. Hemodynamic characteristics, myocardial kinetics and microvascular rheology of FS-069, a second-generation echocardiographic contrast agent capable of producing myocardial opacification from a venous injection. J Am Coll Cardiol 1996;28:1292–300.
28. Wei K, Skyba D, Firschke C, Jayaweera AR, Lindner JR, Kaul S. Interactions between microbubbles and ultrasound: in vitro and in vivo observations. J Am Coll Cardiol 1997:1081–8.
29. Mulvagh SL, Foley DA, Aeschbacher BC, Klarich KK, Seward JB. Second harmonic imaging of a intravenously administered echocardiographic contrast agent: visualization of coronary arteries and measurement of coronary blood flow. J Am Coll Cardiol 1996;27:1519–25.
30. Firschke C, Lindner JR, Goodman NC, Skyba D, Wei K, Kaul S. Myocardial contrast echocardiography in acute myocardial infarction using aortic root injections of microbubbles in conjunction with harmonic imaging: potential application in the cardiac catheterization laboratory. J Am Coll Cardiol 1997;29:207–16.
31. Porter TR, Xie F, Kilzer K. Intravenous perfluoropropane-exposed sonicated dextrose albumin produces myocardial contrast which correlates with coronary blood flow. J Am Soc Echocardiogr 1995;8:710–8.
32. Porter TR, Xie F, Kricsfeld D, Armbruster RW. Improved myocardial contrast with second harmonic transient ultrasound response imaging in humans using intravenous perfluorocarbon-exposed sonicated dextrose albumin. J Am Coll Cardiol 1996;27:1497–501.
33. Wei K, Jayaweera AR, Firoozan S, Linka A, Skyba DM, Kaul S. Quantification of myocardial blood flow with ultrasound-induced destruction of microbubbles administered as a constant venous infusion. Circulation 1998; 97:473–83.